Available online at www.sciencedirect.com
ScienceDirect
Journal of Nuclear Materials 363–365 (2007) 196–200
journal of nuclear materials
www.elsevier.com/locate/jnucmat

Divertor heat flux scaling with heating power and plasma current in H-mode discharges in the national spherical torus experiment

R. Maingi [a,*], C.E. Bush [a], R. Kaita [b], H.W. Kugel [b], A.L. Roquemore [b], S.F. Paul [b], V.A. Soukhanovskii [c], NSTX Team

[a] *Oak Ridge National Laboratory, Oak Ridge, TN, USA*
[b] *Princeton Plasma Physics Laboratory, Receiving 3, Route 1 North, Princeton, NJ 08543, USA*
[c] *Lawrence Livermore National Laboratory, Livermore, CA, USA*

Abstract

We present the first results of lower divertor heat flux scaling with input power (P_{NBI}) and plasma current (I_p) in H-mode discharges in the National Spherical Torus Experiment. These experiments were conducted with $0.6 \leqslant I_p \leqslant 0.9$ MA, $1 < P_{NBI} < 6$ MW, on-axis toroidal field $B_t = 0.45$ T, in a lower-single null discharge shape with elongation $\kappa \sim 2.0$, triangularity $\delta \sim 0.45$, and the ion grad-B drift toward the X-point. As P_{NBI} was raised from 1 MW to 6 MW, the outer divertor peak heat flux was observed to increase up to 6 MW/m^2. A break in the slope of peak heat flux vs. power was observed at heating power ~3 MW, which we interpret as the transition of the divertor toward the high recycling regime and well away from the detachment threshold. The peak heat flux was also observed to increase strongly with I_p.

PACS: 52.55.Fa; 52.40.Hf

Keywords: NSTX; Divertor plasma; Detachment; Target profiles; Sol plasma

1. Introduction

Heat flux management is an important concern in high power density systems. Owing to their compact nature, spherical tori (ST) have the potential for high heat flux at divertor target plates because of the large ratio of P/R, where P is the heating power and R is the major radius of the device. High heat fluxes can be intensified by the relatively short outboard connection length in STs. Fortunately, the ST scrape-off layer (SOL) can be designed to have high poloidal flux expansion at the target, which has been shown to reduce the peak heat flux [1]. While substantial experimental work has been done in heat flux scaling for higher aspect ratio tokamaks such as DIII-D [2], there are far fewer published reports from lower aspect ratio, spherical tokamaks [3–5].

* Corresponding author. Fax: +1 609 243 2874.
E-mail addresses: rmaingi@pppl.gov (R. Maingi), vlad@ppp.gov (V.A. Soukhanovskii).

0022-3115/$ - see front matter © 2007 Elsevier B.V. All rights reserved.
doi:10.1016/j.jnucmat.2007.01.063

In this paper, we present the first results of outer divertor heat flux scaling with neutral beam heating power (P_{NBI}) and plasma current (I_p) in H-mode discharges in the National Spherical Torus Experiment (NSTX). This work builds upon previous NSTX reports of the peak heat flux scaling in L-mode discharges [6], and power accountability [7] and initial surveys of the heat flux characteristics [8] in H-mode discharges, as well as studies of heat flux management through radiation and detachment [9]. We focus on the outer divertor because the inner divertor remains detached through most of the operational window in NSTX [10].

2. Experiment setup and results of scaling studies

The heat flux profile is measured in NSTX with infrared cameras; the basic method is described here and details are provided elsewhere [11]. The camera is a commercial 12-bit, 30 Hz micro-bolometer camera with sensitivity in the 8–12 μm range and a measured thermal response time constant of ~20 ms. The lower divertor tile infrared emission is calibrated during in situ high temperature bakes, and the heat flux profile is computed from a 1-D conduction model into a semi-infinite solid [2], i.e. neglecting thermal transport along the surface of the tile.

The lower single-null diverted discharges used in this study had the following parameters: $0.6 \leqslant I_p \leqslant 0.9$ MA, $1 \leqslant P_{NBI} \leqslant 6$ MW, toroidal field on-axis $B_t = 0.45$ T, elongation $\kappa = 2.0$, average triangularity $\delta \sim 0.45$, and a large inner-wall gap between 6 and 10 cm. The temporal evolution of the highest power discharge used in the P_{NBI} scan is shown in Fig. 1. Neutral beam heating during the I_p ramp was used to minimize volt-second consumption during the ramp-up. As in most NSTX H-mode discharges, the line-average density (n_e^{FIR}) ramped throughout the discharge, owing partly to continuous gas fueling from the high-field side gas injector which improves the reliability of H-mode access in STs [12,13]. The stored energy (W_{MHD}) continued to increase slowly after the L–H transition at 0.22 s, until it was clamped at the onset of Type I edge-localized modes (ELMs) at $t = 0.345$ s.

2.1. Outer divertor heat flux scaling with P_{NBI}

The scaling of peak divertor heat flux with P_{NBI} was conducted with constant $I_p = 0.8$ MA over a range of $1 \leqslant P_{NBI} \leqslant 6$ MW. To insure reliable H-mode transitions, all discharges had $P_{NBI} = 4$ MW until ~0.23 s, after which the power was changed to the desired level by 0.26 s. As previously reported [14], the ELM character changed substantially during the P_{NBI} scan upon reaching a critical value of normalized beta $\beta_N \sim 5$ [$\beta_N \equiv (\beta_t a B_t / I_p)$ where toroidal beta $\beta_t = 2\mu_0 W_{MHD}/B_t^2$, a is the minor radius, and W_{MHD} is the plasma stored energy]. Fig. 2 shows that below 4 MW of heating power, the discharges had only small, Type V ELMs [15] and no Type I ELMs. For $P_{NBI} \geqslant 4$ MW, a mixture of Type V and Type I ELMs were observed, with the Type I ELM frequency increasing with P_{NBI}. These Type I ELMs individually resulted in a stored energy drop between 4% and 10%, consistent with previous NSTX Type I ELM scaling studies [16]. The impact of the large ELMs on the heat flux profile was modest, however, owing to the long frame integration time of 33.3 ms relative to the typical ELM time scale of 1–2 ms. An analysis window of 110 ms (four camera frames) was used to minimize the impact of the large ELMs on the heat flux profiles. During this time window, it should be noted that the line-averaged density typically increased by 20–25%.

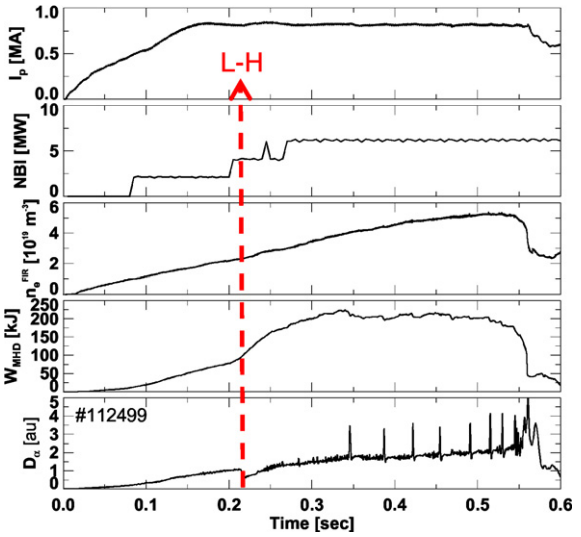

Fig. 1. Time traces of highest heating power discharge. Density ramps throughout the discharge, due partly to continuous gas fueling from the center stack region. Note that the stored energy comes into equilibrium, and the discharge exhibits both small Type V ELMs and large Type I ELMs.

As shown in Fig. 3, the peak heat flux Q_{peak} increased with the power flowing into the SOL, P_{loss}. Here loss power is defined as $P_{loss} = P_{OH} + P_{NBI} - dW_{MHD}/dt - P_{rad}^{core} - P_{loss}^{fast\ ion}$, where P_{OH} is

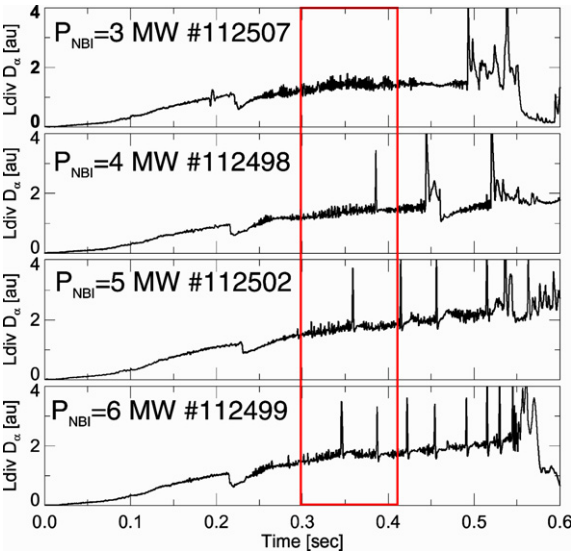

Fig. 2. Dependence of ELM activity on heating power at constant $I_p = 0.8$ MA. At low heating power, only Type V ELMs are observed. The frequency of type I ELMs increased with the heating power. The time window of the analysis is shown by the red box. (For interpretation of the references in colour in this figure legend, the reader is referred to the web version of this article.)

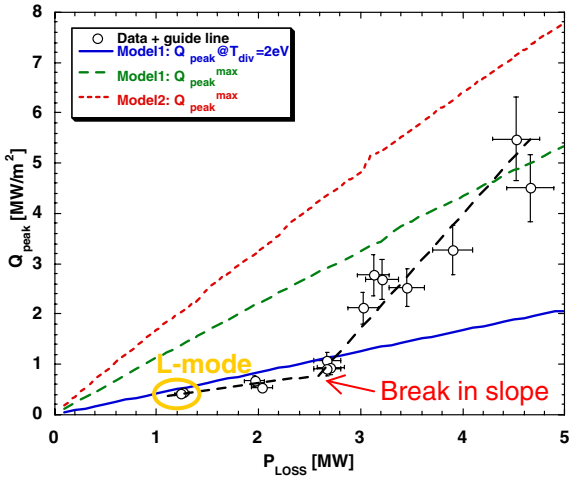

Fig. 3. Dependence of outer divertor peak heat flux (open circles) on SOL loss power. The dashed black lines are lines to guide the eye, and the other lines are predictions from the Borass model (see the text).

the ohmic heating power, $P_{\text{rad}}^{\text{core}}$ is the core radiated power, and $P_{\text{loss}}^{\text{fast ion}}$ is the fast ion loss. From our power accounting study [7], we use that $P_{\text{rad}}^{\text{core}} \sim 0.1(P_{\text{OH}} + P_{\text{NBI}})$ and $P_{\text{loss}}^{\text{fast ion}} \sim 0.2(P_{\text{OH}} + P_{\text{NBI}})$. A change in the slope is evident for P_{loss} between 2.5 and 3 MW, i.e. Q_{peak} began to increase much more quickly. We note that the discharges reverted back to L-mode at the very lowest P_{loss} as it was below the H–L threshold at the operating densities in those discharges.

To obtain insight into the experimental trends, these data were simulated with a two-point model of the SOL derived by Borass et al. [17]. While this model was originally proposed to simulate SOL induced density limits in tokamaks, it nevertheless provides a useful framework for the operating window in tokamak and ST SOLs. The model was previously used for DIII-D detachment studies with only minor modifications [18], and the basic implementation for NSTX follows along the lines of that study. In the model equations, the heat flux can be parameterized as a function of assumed divertor temperature, either for a fixed SOL power flux width at the outer midplane or one computed from a cross-field transport scaling, such as Bohm transport. The relevant model inputs used for NSTX are given in Table 1.

Three curves from the two-point model calculations are shown in Fig. 3. The solid blue line[1] corresponds to a fixed SOL upstream heat flux width of 1.5 cm for an assumed divertor temperature of 2 eV, i.e. just above the onset of partial detachment observed in tokamaks [19]. The dashed green line corresponds to the maximum heat flux computed for the entire range of divertor temperatures considered, with the upstream SOL width fixed at 1.5 cm as above. Finally the dotted red line corresponds to the maximum heat flux computed for the range of divertor temperatures considered, with the assumption of Bohm level cross-field transport to self consistently compute the SOL width.

The main difference between the solid green and dashed blue curves originates from the enhanced carbon divertor radiation computed at a divertor temperature of 2 eV, as compared with higher temperatures typically between 20 and 40 eV, where the maximum heat flux is predicted to occur. Practically this difference is realized by variation of the upstream density through fueling variations. The main difference between the dashed green line and the dotted red line is that the SOL width is typically narrowed as the SOL temperature increases, i.e. the predicted SOL heat flux width for Bohm transport

[1] For interpretation of color in Fig. 3, the reader is referred to the web version of this article.

Table 1
NSTX input parameters used for the two-point model results shown in Fig. 3

Major radius (m)	0.86
Minor radius (m)	0.63
Elongation	2.0
Field on axis (T)	0.45
Plasma current (MA)	0.8
Carbon impurity fraction in divertor	0.05
$\alpha_{q\perp}$, α_{DBohm}	1.1
q_{cyl} (for connection length)	2.0
η (fraction of SOL power to low field side)	0.75

shrunk to 1.1–1.3 cm from the assumed fixed width of 1.5 cm in the other cases.

From these calculations, we can judge that the outer divertor was probably close to detachment at the lowest power levels, and that the sharp change in slope corresponds to the onset of the high recycling conduction-limited regime [20], as the SOL moves toward the sheath limited regime. Indeed the peak heat flux was measured to be <1 MW/m^2 at the lower power levels, approaching the values observed in radiative and detached divertor studies in NSTX [9]. The fact that the data lie *below* the solid blue line, which represents detachment onset, is perhaps not surprising, given that the power accountability in these discharges was 70% at the higher power levels and down to 60% at the lowest power levels [7]. Including an anomalous power loss of 30–40%, the solid blue line would shift below the data, representing a lower bound as expected.

2.2. Outer divertor heat flux scaling with plasma current

The scaling of peak divertor heat flux with plasma current was conducted with constant $P_{NBI} = 4$ MW over a range of $0.6 \leqslant I_p \leqslant 0.9$ MA. Small variations in P_{OH} and dW_{MHD}/dt resulted in a P_{loss} range between 3.0 and 3.5 MW during the scan. As in the P_{NBI} scan, all discharges had a secular density ramp during the analysis time window of 0.3–0.41 s.

The time evolution of the lower divertor D_α is shown in Fig. 4 for representative discharges of the I_p scan. A tendency toward large ELMs was observed as the I_p was increased at fixed P_{NBI}. Small Type V ELMs were also present in all of the discharges.

The outer divertor peak heat flux increased strongly with I_p from 0.6 to 0.9 MA, as shown in Fig. 5. Correspondingly the heat flux profile width (full-width at half-max value) decreased with

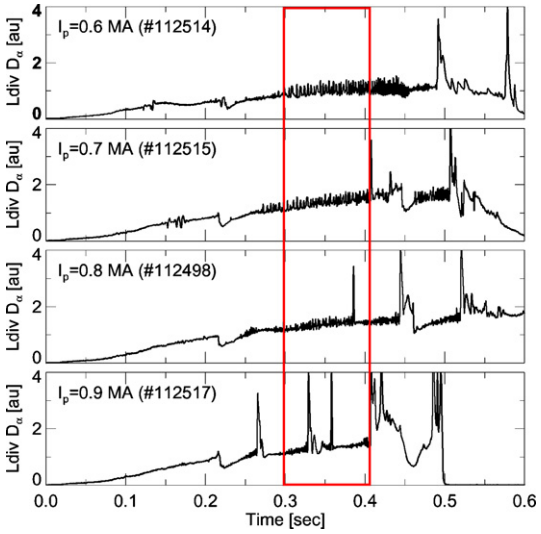

Fig. 4. Dependence of ELM activity on I_p at constant $P_{NBI} = 4$ MW. Type I ELMs are observed at $I_p \geqslant 0.7$ MA. The time window of the analysis is shown by the red box. (For interpretation of the references in colour in this figure legend, the reader is referred to the web version of this article.)

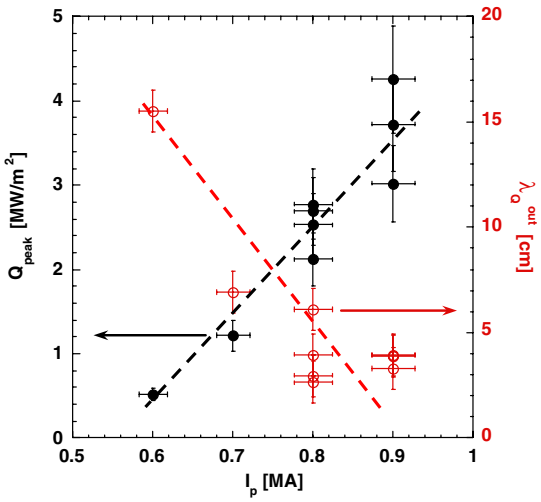

Fig. 5. Dependence of outer divertor peak heat flux and profile width on I_p. The peak heat flux (width) increases (decreases) rather strongly with I_p. The black and red dashed lines are placed solely to guide the eye and should not be used to extrapolate the dependencies outside of the dataset ranges. (For interpretation of the references in colour in this figure legend, the reader is referred to the web version of this article.)

increasing I_p from 0.6 to 0.8 MA. More data are required to determine if the width dependence extends to $I_p \geqslant 0.9$ MA. This observed dependence of the peak heat flux and width on I_p is stronger than suggested by the simple two-point model

discussed above. We note, however, that a strong increase of Q_{peak} with I_p has been previously observed experimentally and reproduced with a model which predicted that the cross-field SOL width would decrease with increasing I_p, leading to a more peaked profile [21].

3. Summary and conclusions

We have presented the first measurements of the scaling of the outer divertor peak heat flux with input power and plasma current in the NSTX. We find that peak heat flux increased with heating power, and that the rate of increase accelerated at the higher power levels. A two-point model was used to simulate the data, from which we conclude that the sharp increase in the dependence can be attributed to the divertor plasma movement into the high recycling regime away from the detachment threshold.

We have also shown that the peak heat flux increased strongly with I_p, and that the width decreased over most of the available I_p scan. The dependence is stronger than that predicted by the two-point model if the sole impact of I_p is on the SOL connection length. More work is required to quantify the impact of the higher I_p on reducing the SOL cross-field transport, which would naturally lead to a smaller heat flux width.

Acknowledgements

This research was supported by the US Department of Energy under contracts DE-AC05-00OR22725, DE-AC02-76CH03073, and W-7405-ENG-48. We gratefully acknowledge the contribution of the NSTX technical staff and operations staff, and the assistance of Charles Lasnier of Lawrence Livermore National Laboratory in the heat flux calculations.

References

[1] D.A. Gates, R. Maingi, J.E. Menard, et al., Phys. Plasmas 13 (2006) #056122.
[2] C.J. Lasnier et al., Nucl. Fusion 38 (1998) 1225.
[3] J.-W. Ahn et al., J. Nucl. Mater. 290–293 (2001) 820.
[4] G.F. Counsell et al., Plasma Phys. Control. Fus. 44 (2002) B23.
[5] G.F. Counsell et al., Plasma Phys. Control. Fus. 44 (2002) 827.
[6] R. Maingi et al., J. Nucl. Mater. 313–316 (2003) 1005.
[7] S.F. Paul et al., J. Nucl. Mater. 337–339 (2005) 251.
[8] R. Maingi et al., Nucl. Fusion 43 (2003) 969.
[9] V.A. Soukhanovskii et al., J. Nucl. Mater. (2007).
[10] V.A. Soukhanovskii et al., J. Nucl. Mater. 337–339 (2005) 475.
[11] D.M. Mastrovito et al., Rev. Sci. Instrum. 74 (2003) 5090.
[12] A.R. Field et al., Plasma Phys. Control. Fus. 46 (2004) 981.
[13] R. Maingi et al., Plasma Phys. Control. Fus. 46 (2004) A305.
[14] R. Maingi, C.E. Bush, E.D. Fredrickson, et al., Nucl. Fusion 45 (2005) 1066.
[15] R. Maingi, K. Tritz, E. Fredrickson, et al., Nucl. Fusion 45 (2005) 264.
[16] R. Maingi, S.A. Sabbagh, C.E. Bush, et al., J. Nucl. Mater. 337–339 (2005) 727.
[17] K. Borass et al., Nucl. Fusion 31 (1991) 1035.
[18] R. Maingi et al., J. Nucl. Mater. 266–269 (1999) 598.
[19] C.S. Pitcher et al., Plasma Phys. Control. Fus. 39 (1997) 779.
[20] M.A. Mahdavi et al., Phys. Rev. Lett. 47 (1981) 1602.
[21] D.N. Hill et al., J. Nucl. Mater. 196–198 (1992) 204.